



# sUAS NOISE CHARACTERISATION DURING HOVERING OPERATIONS

Carlos Ramos-Romero<sup>1\*</sup> Nathan Green<sup>1</sup>  
César Asensio<sup>2</sup> Antonio J Torija<sup>1</sup>

<sup>1</sup> Acoustics Research Centre, University of Salford, Manchester M5 4WT, UK.

<sup>2</sup> Instrumentation and Applied Acoustics research group (I2A2),  
Universidad Politécnica de Madrid, Madrid 28031, Spain.

## ABSTRACT

In the framework of the EPSRC - UK DroneNoise project, a multi-channel methodology for small Unmanned Aircraft Systems (sUAS) noise measurement was applied under controlled conditions. The measurement campaign was carried out in August 2022 in Edzell, a village in Scotland. This paper presents preliminary results on the application of this on-field measurement protocol for a series of sUAS during hovering. Noise signals were recorded from two quadcopters and one hexacopter in stationary flight using a linear ground microphone array. The data were then analysed in both time and frequency domains. In addition, back-propagation techniques were applied for the calculation of noise directivity. Comparisons of the acoustic footprint of the tested sUAS were carried out using both acoustic metrics and Sound Quality Metrics (SQMs). The analysis procedure presented in this paper can also report SQMs at different receivers to aid the psychoacoustic assessment of sUAS noise.

**Keywords:** *sUAS noise, on-field noise measurements, Sound Quality Metrics.*

## 1. INTRODUCTION

Since the introduction of new multi-rotor aircraft flying close to the community, the study of their emitted noise is considered a key part of the public acceptance criteria

*\*Corresponding author: C.A.RamosRomero@salford.ac.uk.*

**Copyright:** ©2023 First author et al. This is an open-access article distributed under the terms of the Creative Commons Attribution 3.0 Unported License, which permits unrestricted use, distribution, and reproduction in any medium, provided the original author and source are credited.

for the successful adoption of small Unmanned Aircraft Systems (sUAS) in the airspace [1].

Due to the versatile flight capabilities, characterising the noise footprint of sUAS is a challenging task, which also increases in complexity when the aircraft is highly affected by adverse weather conditions during operations (*e.g.*, wind gusts). The noise emission of sUAS varies depending on the specific operating conditions, and therefore the acoustics characterisation and analysis of these vehicles separately consider four types of flight operations: take-off, hovering, flyover, and landing [2, 3].

In particular, for hovering operations, the recently published EASA “*Guidelines on Noise Measurement for Unmanned Aircraft Systems*” recommend reporting the equivalent continuous sound level  $L_{Aeq}$  as the main acoustic metric to quantify the overall sound pressure level of each sUAS event [4].

On the other hand, Sound Quality Metrics (SQMs) describe the psychoacoustic characteristics of signals that are useful from a noise perception perspective. This concept is important because sUAS noise has been credited as more annoying than conventional aircraft noise at the same loudness level, and sUAS noise annoyance is significantly related to loudness, sharpness, and fluctuation strength [5, 6].

This paper presents the results of the acoustic characterisation of sUAS during hovering, using the  $L_{Aeq}$  metric and the derivation of directivity of the main noise components. This approach includes the noise level contributions from broadband noise and tonal components, which includes the shaft frequencies, blade passing frequencies (BPF), and their harmonics. Furthermore, a psychoacoustic characterisation of the sUAS tested during hovering is also presented.



## 2. METHODS

The sensing setup considered nine free-field microphones mounted on metal ground plates placed in a straight line (Fig. 1<sup>1</sup>). Each microphone position was derived to obtain steps of  $\Delta\Theta = 15^\circ$  to each side of the centre microphone over which the sUAS hovered at 10 m height. The experimental setup was also applied for noise characterisation during flyovers in [7] following the recommendations of the ISO working group and NASA-UNWG [8,9].

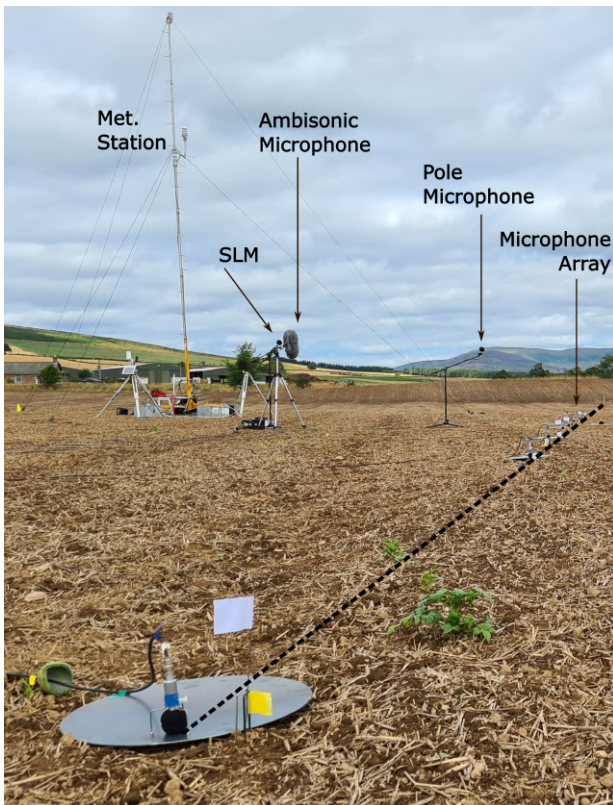


**Figure 1.** Sensing setup

Noise levels were reported as  $L_{Aeq}$  at each microphone position. Furthermore, a frequency analysis allowed extracting the noise contribution from narrow-band components and/or the overall sound pressure levels.

<sup>1</sup>This paper only reports data from the microphone array at ground level. The Sound Level Meter, Ambisonic microphone, and pole-mounted microphone were included for further research proposes.

**Table 1.** sUAS basic info

Model	sUAS ID	Number of rotors	Weight [g]	Diagonal Wheelbase [mm]	Payload Weight [g]
DJI Matrice 300 RTK	M3	4	6300	895	930
Yuneec H520E	Yn	6	1633	520	350
DJI Mini 3 pro	3p	4	249	247	-

To obtain the noise directivity of each sUAS, the sound pressure levels recorded on the ground were back-propagated to the constant radius centred at sUAS position  $r_0 = 1$  m. This process was carried out considering the effects of atmospheric absorption, spherical spreading [10], and pressure doubling from the free-field condition [11].

In addition, SQMs were also derived at each microphone position to investigate the differences in the psychoacoustics attributes of noise emitted by each sUAS tested.

### *Aircraft description and operation*

Hovering is a sUAS flight operation where the aircraft stays in a stationary position. For this study, the sUAS hovered above the centre microphone during 20 s. The noise recordings of the three multi-rotor sUAS described in Tab. 1 were included in the database [12] for analysis.

## 3. RESULTS

### *Acoustic metrics.*

The averages of the instantaneous A-weighted sound pressure level  $L_A$  of three hovering events, for each of the tested sUAS are presented in Fig. 2.

The highest amplitudes correspond to the drone (M3) with and without the corresponding payload attached (Tab. 1). The sound levels produced by the other sUAS (Yn and 3p) showed a lower values of  $L_A$ . As expected, hover operations are stationary during the recorded time, as shown in Fig. 2. However, the smaller sUAS seems to have a more unstable behaviour which has an impact on the sound emissions (see the 2 seconds at the beginning of the time frame in Fig. 2). This sUAS seems to be more affected by weather conditions, piloting causes or remote control problems.

The  $L_{Aeq}$  metric was then calculated at each microphone position. Since the sUAS hovers above the centre microphone position (5<sup>th</sup> microphone), the decreasing

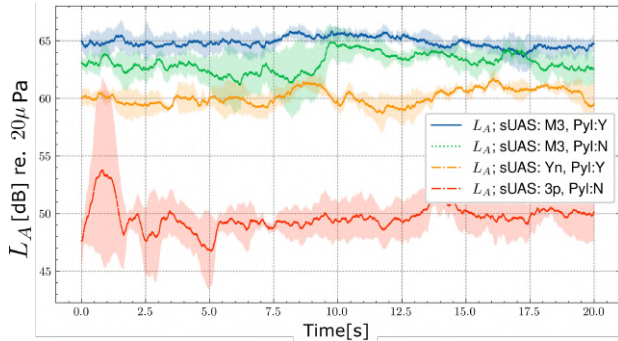


**Figure 2.** Instantaneous  $L_A$  during hovering of sUAS at centre microphone.

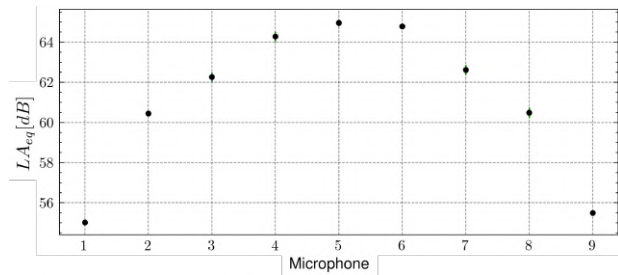


**Figure 3.**  $L_{Aeq}$  on all microphone positions during hovering. sUAS: M3 with payload attached

amplitude is presented symmetrically on each side of the microphone array in Fig. 3.

Recorded sound signals were analysed in the frequency domain to extract the tonal and broadband (assumed to be mainly trailing edge noise) components.

Fig. 4 shows the Power Spectral Density (PSD, in dB/Hz) for the M3 sUAS during hovering. For this specific sUAS, the first series of tonal components correspond to the shaft frequencies (around 40 Hz), then the rotors' Blade Passing Frequencies (BPFs) are located about 100 Hz. The rotors' BPFs harmonics are very consistent between the three hovering events for the M3 sUAS.

The stability (in time) of the sound signals, and specifically the tonal components, of the sUAS tested can be observed in a spectrogram. For instance, Fig. 5 shows how the tonal components of the M3 sUAS are very stable during 20 s of measurement. However, as shown in Fig. 2, the stability of the sound signals depends on the size of the aircraft and even more on the influence of weather conditions [13].

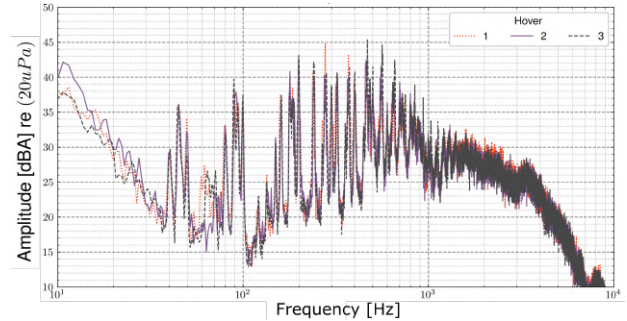


**Figure 4.** PSDs of three recordings at centre microphone during hovering. sUAS: M3 with payload attached

The frequency range depicted (below 1000 Hz) is the region where the tonal components appear to be dominant.

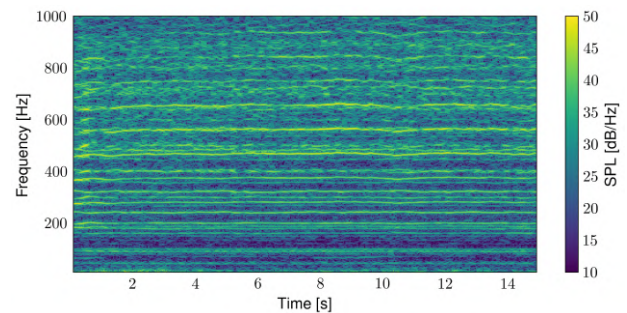


**Figure 5.** Spectrogram at centre microphone position during hovering. sUAS: M3 with payload attached

The decomposition process into tonal and broadband components can be performed on each microphone data using a moving-median filter of the spectra [14]. The tonal component is then considered as the contribution of the prominent peaks (at least  $\geq 6$  dB than the median-filtered spectrum). For the hovering event presented in Fig. 6 (M3 uUAS, at the centre microphone) broadband noise is the dominant component (in the high frequency region), closer to the  $L_{Aeq}$  amplitude, and therefore  $\approx 10$  dB higher than the tonal component. The frequency range for the integration of SPL was established from 50 Hz to 1000 Hz. At low-to-mid frequencies, tonal noise (*i.e.*, shaft frequencies, BPFs and BPFs' harmonics) dominates the frequency spectrum.

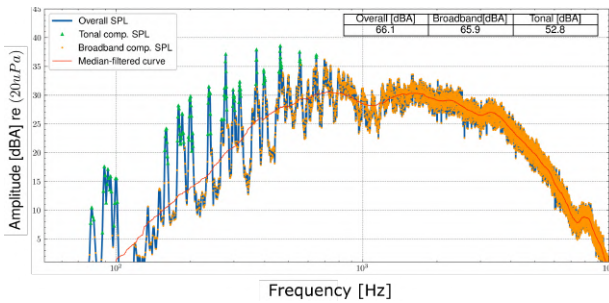


**Figure 6.** sUAS noise components: Overall, Tonal and Broadband derived at centre microphone position during hovering. sUAS: M3 with payload attached

### Directivity.

The directivity of tonal and broadband noise components, and overall noise levels were calculated by back-propagating the sound level amplitudes from the nine ground microphone array data to a position  $r_0 = 1$  m from the sUAS. The microphone positions provided the sound level at angles  $-60^\circ \leq \Theta \leq 60^\circ$ .

Fig. 7 shows the directivities of broadband and tonal components for the M3 sUAS. Broadband noise directivity shows directional emission at sUAS underneath position, with lower amplitude ( $\approx -5$  dB) at extreme angles ( $-60^\circ$  and  $60^\circ$ ).

The tonal component shows differences in sound levels from the broadband component higher than 10 dB in most of the angles, with also a more directional emission towards the emission angles beneath the sUAS. The directivity of the overall A-weighted sound level closely matches the directivity of the broadband noise component. This is mainly due to the broadband noise component dominating the mid-to-high region in the frequency spectrum of the M3 sUAS. This is also another indication of the potential issue of the impact of high-frequency broadband noise on sUAS noise perception, especially when the vehicle is operating at a close distance from communities.

Gwak et al., [5] pointed out the concentration of acoustic energy in the high-frequency region as one of the main differences between the noise signature of sUAS and other conventional civil aircraft.

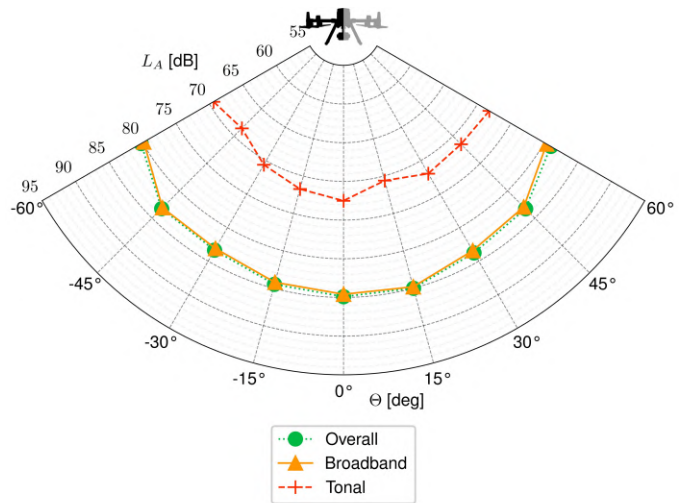


**Figure 7.** sUAS Horizontal Directivity: Overall, Tonal and Broadband components during hovering. sUAS: M3 with payload attached

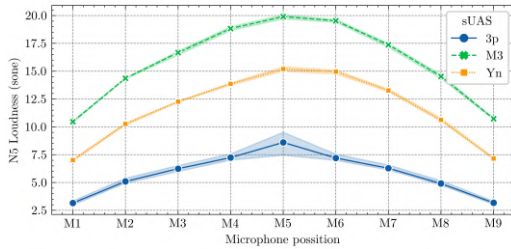
### Sound Quality Metrics.

In addition to the above acoustic characterisation, a psychoacoustic characterisation was performed by using a series of SQMs. The three SQMs chosen are: Loudness, Sharpness and Fluctuation Strength. These SQMs were selected as they are highly correlated with sUAS noise annoyance [5, 6]. The SQMs were calculated with the software HEAD Acoustics ArtemiS SUITE 12.0. The exceedance level of 5% was calculated for a set of SQMs. The level of exceedance represents the highest SQM value reached during the recorded events.

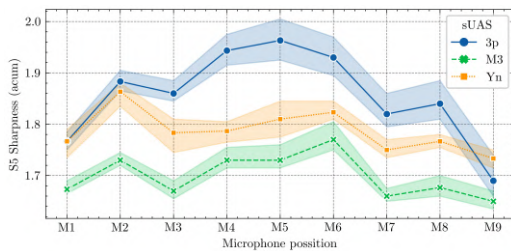
Fig. 8 depicts the mean value of each SQM for all the hovering events at the receiver positions, for each sUAS. Specifically, the 5<sup>th</sup> percentile and the inter-quartile range of Loudness (human perception of sound volume, in [sones]), Sharpness (the perception of the greater proportion of high frequency content of a sound, in [acum]), and Fluctuation Strength (the perception of the very-low frequency variation of the signal amplitude or frequency, in [vacil]).

The Loudness metric (Fig. 8-a) seems to be directly related to the sUAS size, with higher values at centre microphone position and decreasing towards both sides of the microphone array.

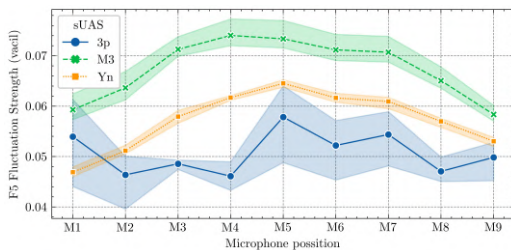
The Sharpness metric (Fig. 8-b) is higher for the smallest sUAS. The sUAS 3p has the highest unbalanced of noise content towards the high-frequency region. In this



(a) N5 Loudness



(b) S5 Sharpness



(c) F5 Fluctuation Strength

**Figure 8.** Sound Quality Metrics during. The interquartile range is also depicted.

case, the value of Sharpness seems to be inversely related to the size of the sUAS.

Finally, the Fluctuation Strength metric (Fig. 8-c) shows that the amplitude modulation due to the interaction between rotors is higher for the biggest sUAS (M3) than the small ones. Likewise, low-frequency modulated amplitude was clear visualised in the BPF range for the sUAS M3 during flyovers [7].

#### 4. CONCLUSIONS

A multi-channel array method for the sUAS characterisation of acoustic and psychoacoustic parameters has been successfully applied to three sUAS varying in size (and payload).

Post-processing of measured sound signals and fur-

ther calculations of acoustic metrics and SQMs allow us to provide a complete characterisation of the sUAS tested. This includes information about spectral, temporal and directivity characteristics, which are highly correlated to sUAS noise perception.

This experimental setup provides a useful tool to obtain the noise characteristics of sUAS under real operations, and can contribute to the development of protocols for sUAS noise certification. A complete acoustic (and psychoacoustic) characterisation can also contribute to the development of policy-making for public acceptance.

Some opportunities have been identified to improve the capabilities of the method, such as including measurements from yaw maneuvers and hovering at greater heights above ground level, and also other arrangements of the microphone array to minimise generated air flow impinging on the ground microphones.

#### 5. ACKNOWLEDGMENTS

The authors C.Ramos-Romero, N. Green and A.J. Torija acknowledge the EPSRC-UK funding for DroneNoise project (EP/V031848/1). C. Asensio acknowledges the funding of the "José Castillejo" Mobility Programme from the Ministry of Universities - Spain. All authors wish to acknowledge the support provided by partners DTLX, Edinburgh Drone Company, and Hayes McKenzie Consultants.

#### 6. REFERENCES

- [1] R. Aalmoes, M. Tojal Castro, N. Sieben, and R. Roosien, "Drone noise in my backyard: the challenges for public acceptability," in *INTER-NOISE 2022 Congress*, Institute of Noise Control Engineering, 2022.
- [2] D. R. Read, D. A. Senzig, C. J. Cutler, E. Elmore, H. He, *et al.*, "Noise measurement report: Unconventional aircraft-choctaw nation of oklahoma: July 2019," tech. rep., John A. Volpe National Transportation Systems Center, :Cambridge, MA, US, 2020.
- [3] N. B. Konzel and E. Greenwood, "Ground-based acoustic measurements of small multirotor aircraft," in *Vertical Flight Society's 78th Annual Forum & Technology Display*, p. 11, Vertical Flight Society, 2022.
- [4] EASA, "Guidelines on Noise Measurement of Unmanned Aircraft Systems Lighter than 600 kg. Operat-

ing in the Specific Category (Low and Medium Risk).  
Public Consultation,” 2022.

- [5] D. Y. Gwak, D. Han, and S. Lee, “Sound quality factors influencing annoyance from hovering UAV,” *Journal of Sound and Vibration*, vol. 489, p. 115651, 2020.
- [6] A. J. Torija and R. K. Nicholls, “Investigation of metrics for assessing human response to drone noise,” *International Journal of Environmental Research and Public Health*, vol. 19, no. 6, p. 3152, 2022.
- [7] C. Ramos-Romero, N. Green, C. Asensio, and A. J. Torija, “On-field measurement for sUAS noise characterization,” in *10<sup>th</sup> Convention of the European Acoustic Association - Forum Acusticum 2023 Proc.*, Italian Acoustical Association, 2023.
- [8] ISO/TC 20/SC 16, “Unmanned aircraft systems,” technical committee, American National Standards Institute, Washington 20036 DC, USA, 2022.
- [9] NASA-UNWG-Subgroup 2, “UAM Ground & Flight Test Measurement Protocol,” 2022. Accessed: 2022-04-11.
- [10] ISO 9613-2:1996, “Acoustics – Attenuation of sound during propagation outdoors – Part 2: General method of calculation,” standard, International Organization for Standardization, Geneva, Switzerland, 1996.
- [11] P. Rasmussen and L. Lars Winberg, “Accurate measurement of drone noise on the ground,” in *QUIET DRONES Second International Symp. on noise from UASs/UAVs and eVTOLs, Paris, France*, p. 11, 2022. INCEEurope, Centre d’information sur le Bruit.
- [12] C. Ramos-Romero, N. Green, C. Asensio, and A. J. Torija, “Dronenoise databse,” Acoustics and Pyschoacoustics metrics database from EPSRC DroneNoise Project EP/V031848/1, Acoustics Research Centre - University of Salford, 2023.
- [13] W. N. Alexander, J. Whelchel, N. Intaratep, and A. Trani, “Predicting community noise of suas,” in *25th AIAA/CEAS Aeroacoustics Conference*, p. 2686, 2019.
- [14] F. Casagrande Hirono, A. Torija Martinez, and A. Elliott, “Optimization of a contra-rotating propeller rig for reduced psychoacoustic impact,” in *INTER-NOISE and NOISE-CON Congress and Conference Proc.*, vol. 265, pp. 4077–4087, Institute of Noise Control Engineering, 2023.